Tellus

ISSN: 0040-2826 (Print) 2153-3490 (Online) Journal homepage: https://www.tandfonline.com/loi/zela19

Some Examples of Stationary Planetary Flow Patterns in Bounded Basins

Henry Stommel, A. B. Arons & A. J. Faller

To cite this article: Henry Stommel, A. B. Arons & A. J. Faller (1958) Some Examples of Stationary Planetary Flow Patterns in Bounded Basins, Tellus, 10:2, 179-187, DOI: 10.3402/tellusa.v10i2.9238

To link to this article: https://doi.org/10.3402/tellusa.v10i2.9238

SVENSKA GEOFYSISKA FÖRENINGEN

VOLUME 10, NUMBER 2 **Tellus** MAY 1958

A QUARTERLY JOURNAL OF GEOPHYSICS

Some Examples of Stationary Planetary Flow Patterns in Bounded Basins[1]

By HENRY STOMMEL, A. B. ARONS and A. J. FALLER

Woods Hole Oceanographic Institution, Massachusetts

(Manuscript received August 22, 1957)

Abstract

A simple regime of fluid flow is defined. This regime can occur in a homogeneous layer of fluid (i) of uniform depth on a rotating sphere and bounded by meridional barriers (ii) of uniform depth on a betaplane and bounded by barriers running north-south (iii) of radially non-uniform depth on a rotating plane and bounded by radial barriers. The essential elements defining the regime are: (a) the flow in the whole layer is steady and geostrophic except and only (b) at the western boundary where a narrow, intense western boundary current is permitted to depart markedly from geostrophy, and (c) the system, which would otherwise be at rest, is driven by a distribution of sources and sinks of fluid (this includes driving agents such as the wind, which can be expressed in terms of source and sink distributions).

Predictions concerning patterns of flow have been deduced from the defined regime and verified experimentally on a rotating model of type (iii). Certain results obtained were by no means intuitively obvious from *a priori* considerations.

Introduction

It is generally recognized that the specific results obtained in theoretical hydrodynamics are not achieved deductively from the general hydrodynamical equations, but on the contrary, are derived deductively only from very much simplified fluid models (or, to say the same thing, an abbreviated set of equations). For example, there is a large range of problems where the so-called perfect fluid idealization proves an adequate representation of what is observed; another range in which laminar viscous flow is adequate. Hydraulic engineers have invented even simpler sets of equations to describe gradually varied flow and flow in transitions. The justification for applying such simplified equations to any particular set of problems is largely *a posteriori;* that is, we judge the reasonableness of the simplified regime of fluid flow by its results.

In meteorology and oceanography there is a constant search for such simple regimes. As an example from meteorology, Rossby's recognition of the essential dynamical elements of the long waves in the westerlies has led to formulation of a barotropic regime of atmospheric flow—and a simple set of equations—which meteorologists hope may describe major features of the atmospheric circulation and perhaps even be useful for prediction. In oceanography there has gradually emerged a conception of a regime of fluid flow which seems to be peculiarly applicable to large scale stationary oceanic flow patterns (for a summary see STOMMEL, 1957). This regime can occur in a homogeneous layer of fluid (i) of uniform depth on a rotating sphere and bounded by meridional barriers (ii) of uniform depth on a beta-plane and bounded by barriers running north-south (iii) of radially non-uniform depth on a rotating plane and bounded by radial barriers. The essential elements which define this simplified regime are: (a) the flow in the whole layer is steady and geostrophic except and only

[1] Contribution No. 939 of the Woods Hole Oceanographic Institution.

(b) at the western boundary where a narrow, intense western boundary current is permitted to depart markedly from geostrophy; and moreover, (c) this system, which would otherwise be at rest, is driven by a distribution of sources and sinks of fluid (various driving agents such as the wind can be expressed in terms of source and sink distributions, so this is no real restriction).

Although our main interest in this regime of planetary flow is in its possible applicability to oceanic circulation, we felt that some of its implications were so bizarre and contrary to intuition that it would be reassuring if they could be partially tested by model experiments. Thus, the model experiments are not meant as »scale models» of what perhaps occurs in the real ocean. We conceive of them as being tests of the internal consistency of the conceptual elements (a, b, c) which define the regime. The notion that such a regime can exist is mainly built on plausibility arguments. The elements which make up the regime are susceptible to quantitative mathematical description; hence, given the distribution of sources and sinks, the circulation pattern can be deduced. If, in comparing the predicted circulation pattern with that observed in a model experiment with a rotating basin, a large discrepancy should arise, it would suggest, among other things, that there were hidden inconsistencies or contradictions in the formulation of the regime. On the other hand, if the experiments with the basin verify the predictions, especially for flow patterns which do not seem intuitively obvious, the belief that such a simple regime might be applicable to the ocean is strengthened, although of course not confirmed. One then, however, feels encouraged to undertake the labor involved in constructing theoretical models and pursuing their implications, the ultimate validation lying in agreement between predictions of the theory and observable phenomena in the ocean.

A priori predictions for a particular rotating model

The model used in this work was a pie-shaped sector of a rotating basin of fluid (Fig. 1). The bottom of the basin is level. The free surface is a paraboloidal cylinder with axis vertical, concave upward. The undisturbed

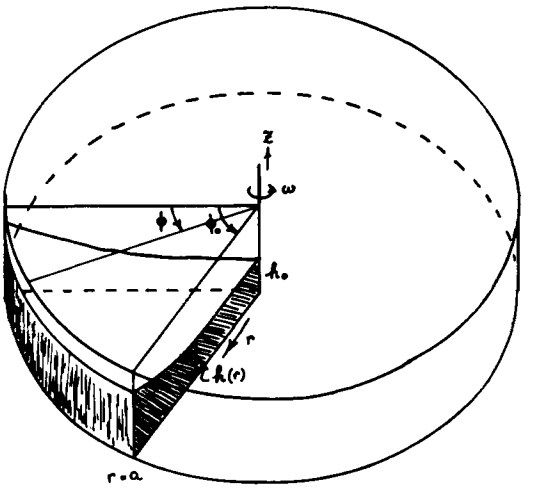

Fig. 1. Schematic diagram of rotating sector showing notation used in theoretical formulation.

depth varies radially from a minimum at the center to a maximum at the rim. The top is covered with a sheet of glass to prevent the air in the room from exerting a stress on the water surface. After the basin has been rotating for some time the fluid in the sector is completely at rest with respect to the basin. In a geometrical configuration of this kind it is clear that any radial component of geostrophic flow is horizontally divergent due to the radial variation in depth of the fluid. A radially outward (inward) component of flow in the interior can therefore only occur if there is a local source (sink) of water. Components of geostrophic flow along circles of constant radius are permissible without divergence, except where blocked by radial barriers.

Before we had carried out any mathematical analysis or experimental work we could see that our regime led qualitatively to some rather remarkable deductions. For example, consider the circulation induced by a point source ⊕ and sink ⊖ of equal intensity placed near to the eastern boundary of the sector (the absolute sense of rotation of the basin in Fig. 2, as viewed from above is counterclockwise, as in the northern hemisphere on the earth) at different radii. Since there are no distributed sources or sinks over the remainder of the basin, all radial geostrophic flow is prohibited in the interior. We deduce that the only permissible circulation pattern, according to the rules of the regime, is one in which zonal geostrophic flow

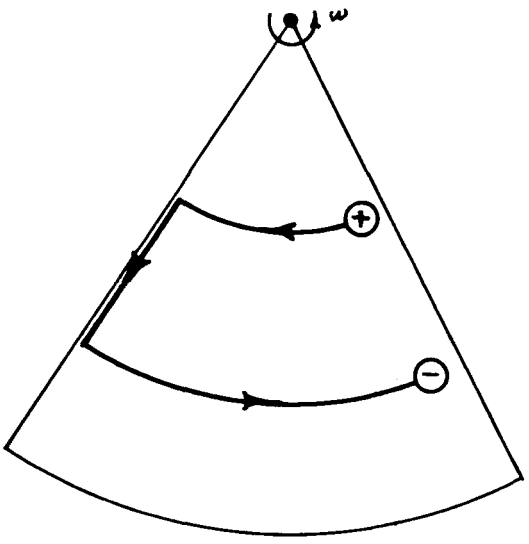

Fig. 2. Diagram of circulation induced in rotating sector by source ⊕ and sink ⊖ positioned as shown.

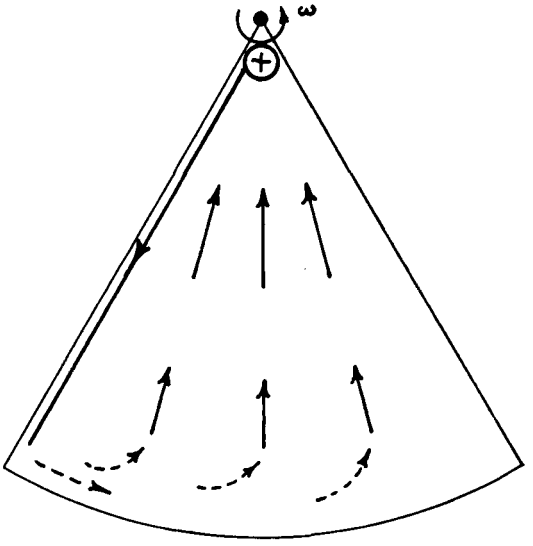

Fig. 3. Sketch of flow pattern expected with source ⊕ at apex of sector, surface of fluid rising uniformly. (Dashed arrows are sketched in to indicate portions of flow not given by elementary theory but evidently required by continuity.)

extends from the source to the western boundary, thence down the western boundary in a narrow, intense boundary current to the radius of the sink, and thence, in another zonal geostrophic flow to the sink. This flow pattern is very circuitous as compared to what occurs in the absence of rotation and non-uniform depth. It was the first flow pattern which we attempted to verify by an actual experiment.

From the point of view of our interest in the eventual application of the regime to oceanic circulation patterns it was desirable to make some deductions and experiments involving distributed sources and sinks. It is easy to obtain a uniform sink (source) over the whole fluid surface by allowing the tank slowly to fill up (empty), thus producing an overall rise (drop) of the free equilibrium surface. As an example, consider the flow pattern induced by an isolated source at the apex of the sector (Fig. 3). Since there is no point sink provided, the free surface rises uniformly—the equivalent of a uniformly distributed sink over the entire sector. Hence, qualitatively, one would expect an inward directed radial component of geostrophic velocity everywhere in the sector, connected to the source by a western boundary current, as sketched in Fig. 3. This is indeed rather surprising: the basin fills up from the rim, although water is added at the apex. But a quantitative analysis (see below) reveals even more surprising features. When the sector is allowed to fill up from an isolated source at the western edge of the rim (Fig. 4), the interior geostrophic flow is again toward the center, but the mathematical development indicates

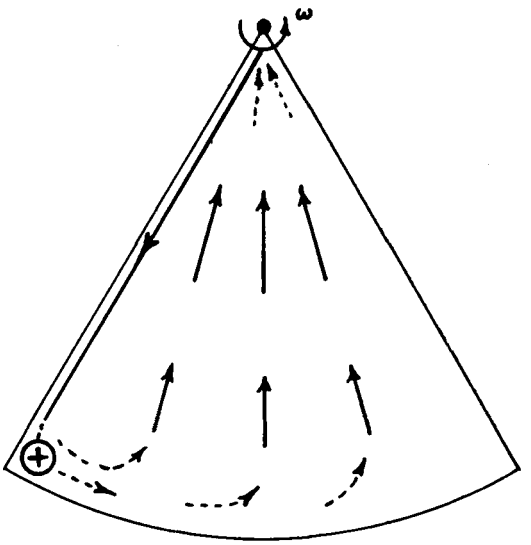

Fig. 4. Sketch of flow pattern expected with source ⊕ at western edge of rim, surface of fluid rising uniformly.

that the interior radial geostrophic transport is so large that it feeds. at the apex, a narrow western boundary current which flows *toward* the source. Such a flow pattern (Fig. 4) is far from being intuitively obvious, but is clearly verified by experiment.

Mathematical analysis

A system of cylindrical coordinates is adopted with notation defined in Fig. 1. The radial pressure gradient associated with the paraboloidal shape of the free surface balances the centripetal acceleration term. We take

$$h = h_0\left(1 + l\frac{r^2}{a^2}\right) \tag{1}$$

$$\text{where } l = \frac{\omega^2 a^2}{2gh_0};$$

h denotes the height of the unpertubed paraboloidal surface. Assuming hydrostatic equilibrium in the vertical direction and denoting by ζ the vertical displacement associated with steady geostrophic flow, the equations of motion (neglecting inertial terms) take the form

$$2\omega v_\varphi = g\frac{\partial \zeta}{\partial r} \tag{2}$$

$$-2\omega v_r = \frac{g}{r}\frac{\partial \zeta}{\partial \varphi} \tag{3}$$

Neglecting ζ relative to h, the equation of continuity is

$$\frac{\partial}{\partial r}(hrv_r) + \frac{\partial}{\partial \varphi}(hv_\varphi) = -r\dot{\zeta} \tag{4}$$

$$\text{where } \dot{\zeta} = \frac{\partial \zeta}{\partial t}$$

Equations (1) throught (4) determine the "interior solution" for the regime we are describing.

Carrying out the differentiation in equation (4):

$$rv_r\frac{dh}{dr} + h\left[\frac{\partial(rv_r)}{\partial r} + \frac{\partial v_\varphi}{\partial \varphi}\right] = -r\dot{\zeta} \tag{5}$$

Cross differentiation and addition of (2) and (3) shows the second term of (5) to be zero. Obtaining $\frac{dh}{dr}$ from (1) and solving for v_r, we have:

$$v_r = -\frac{\dot{\zeta} a^2}{2h_0 l r} \tag{6}$$

Thus the interior geostrophic flow which arises when a source adds water to the basin, producing a positive $\dot{\zeta}$, is northerly directed and has no φ component.

$$\left[\frac{\partial v_\varphi}{\partial \varphi} = -\frac{\partial(rv_r)}{\partial r} = 0, \text{ and } v_\varphi = 0 \text{ at eastern edge.}\right]$$

If sources S (rate of addition of volume) are assumed to produce a uniform vertical rise of the surface throughout the basin, geometrical requirements give the relation:

$$\dot{\zeta} = -\frac{2S}{\varphi_0 a^2}, \tag{7}$$

and equation (6) becomes

$$v_r = -\frac{S}{\varphi_0 h_0 l r} \tag{8}$$

Consider the water budget of the shaded sector defined by $r = r$ in Fig. 5. T_I represents the transport into the sector by the interior geostrophic flow; T_v represents the vertical transport associated with $\dot{\zeta}$; S_0 denotes the source transport; and T_w denotes the western boundary transport. We have postulated the existence of T_w as one of the elements of the regime, and we solve for it on the basis of the mass conservation requirement:

$$T_w + T_I + S_0 + T_v = 0 \tag{9}$$

The ambiguity implied in the term T_w should be carefully noted. This is *not* a dyna-

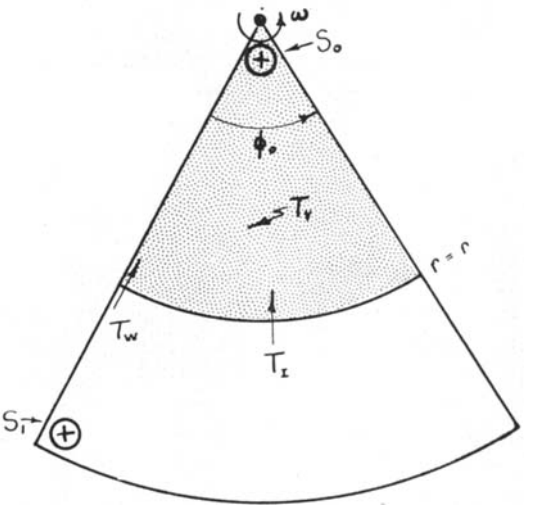

Fig. 5. Notation for analyzing water budget of the shaded sector $T_w + T_I + T_v + S_0 = 0$

mical solution; T_w is simply postulated as a *net* transport. There is nothing in the definition of the regime which precludes more than one stream at the western boundary or meandering of any kind. The net transport may be the result of a single current, of parallel currents in opposite directions, or some other combination.

From equations (7), (8) and the geometry of the system:

$$T_I = -hr\varphi_0 v_r = \frac{S}{l}\left(1 + \frac{lr^2}{a^2}\right) \qquad (10)$$

$$T_v = -\frac{\varphi_0 r^2}{2}\dot{\zeta} = -S\frac{r^2}{a^2} \qquad (11)$$

Solving for T_w:

$$T_w = -\frac{S}{l}\left(1 + \frac{lr^2}{a^2}\right) - S_0 + \frac{Sr^2}{a^2} = -S_0 - \frac{S}{l} \qquad (12)$$

where, for the general case depicted in Fig. 5,

$$S = S_0 + S_1$$

We can now interpret the results for T_w for various specific cases:

Case 1. S_0 positive, $S_1 = 0$. (Fig. 3).
For this case equation (12) becomes:

$$T_w = -S_0\left(1 + \frac{1}{l}\right) \qquad (13)$$

The mathematical analysis of the postulated regime thus predicts a southerly transport at the western boundary of the model. The transport is *larger* than the input of the source at the apex by the amount S_0/l, l being the parameter characterizing the slope of the equilibrium paraboloidal surface. If the angular velocity ω is such that $h(a) = 2h_0$, $l = 1$, and the total boundary transport is *twice* the transport of the source. The transport is independent of r and the boundary current must therefore flow undiminished to the outer rim of the basin, turn to the eastward at the outer rim, and from that region feed the north-bound interior geostrophic flow. Part of the boundary current (the amount S_0/l) represents a *recirculation flow* of water originally in the basin.

Case 2. $S_0 = 0$, S_1 positive (Fig. 4).
For this case equation (12) becomes:

$$T_w = -\frac{S_1}{l} \qquad (14)$$

This predicts a flow pattern essentially similar to that of Case 1, but the result is even more surprising. If $l = 1$, the regime requires a *southerly* boundary current with a transport *equal to that at the source* in the southwest corner! (The same result, of course, is obtained regardless of the position of S_1 along the outer boundary.)

Case 3. $S_0 = -xS_1$, S positive. (i.e. a fraction x of the input is drained off at the apex of the model.)
For this case equation (12) becomes:

$$T_w = \frac{S_1}{l}\left[x(l+1) - 1\right] \qquad (15)$$

In this situation the ambiguity as to the detailed nature of T_w is well dramatized. T_w is only a *net* transport. Thus equation (15) might be interpreted as describing a southerly transport of magnitude $\frac{S_1}{l}$ paralleling a northerly transport $\frac{S_1 x}{l}(l+1)$, or as a single transport either north or south (changing direction when $x = \frac{1}{l+1}$), or as some other combination leading to the same *net* T_w.

Order of magnitude of approximations in the theory

Numerical values for flow, rotation, and basin geometry are given in a later section. Utilizing the numerical data, it can be shown that:

$$\frac{\zeta \text{ max.}}{h} \sim 10^{-4}$$

and that the fractional transport neglected by dropping ζ from the equation for T_I is also of the order of 10^{-4}.

If the sector is cut off at some small radius $r = a_0$ instead of extending to a sharp apex at $r = 0$, equation (12) becomes, to first order terms:

$$T_w = -S_0 - \frac{S}{l} - S\frac{a_0^2}{a^2}\left(1 + \frac{1}{l}\right) \qquad (16)$$

The contribution of the third term on the right hand side is of the order of 10% when a_0/a is about 0.2.

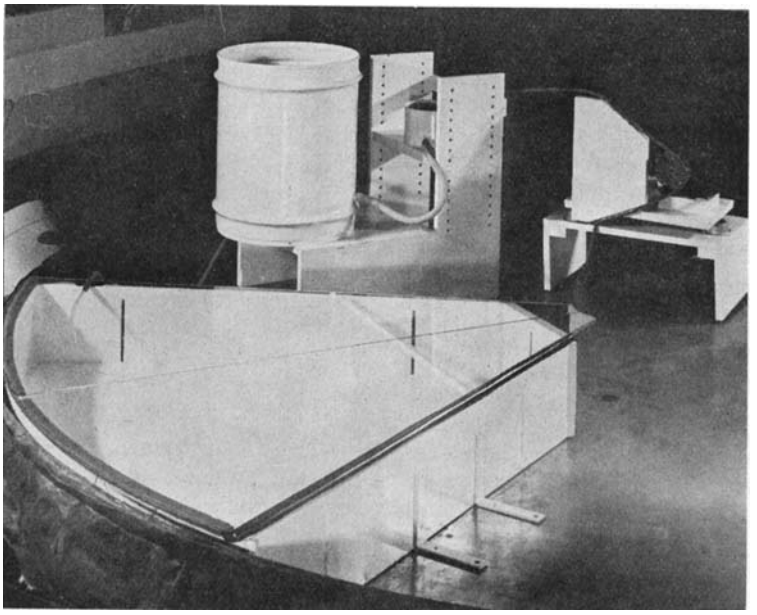

Fig. 6. A photograph of the rotating tank showing the 60° sector with 1/4-inch slots at various positions in the walls for the introduction or extraction of mass. When not in use the slots are sealed with tape. The glass cover prevents wind stress on the free surface of the water. A controlled flow rate is obtained by adjusting the level of the small can (with an overflow) into which water is pumped continuously. A constant head of water is thereby maintained in the large can containing the dyed source water.

The Laboratory Experiments

To check and demonstrate the principles of the foregoing theory and quantitative notions concerning the flow in a simple laboratory model, the 7-ft. diameter rotating tank previously employed for oceanographic models (VON ARX, 1952) was used. For these studies a truncated sector of 60° width (Fig. 6) was isolated by wooden partitions with several vertical slots in the walls for the introduction or extraction of mass. An alternate source was direct injection of the fluid through a vertical glass tube at any desired point in the interior of the sector.

The rate of in flow of mass was an important consideration and was adjusted so that the Rossby number for the western boundary current was of the same order of magnitude as that for the Gulf Stream system. Similar values of the Rossby number (defined by $R_0 = v/\omega R =$ $= .001$ where v is a representative velocity and ωR is the tangential speed of rotation) are obtained when the circulations have approximately the same degree of geostrophy. The ratio of depth at the rim to that at the center (h_a/h_0) was set at approximately 2 in all cases, a value corresponding to $l = 1$ in the theoretical discussion. Other significant parameters were $\omega = 1.05$ sec.$^{-1}$, $a = 100$ cm., and $\bar{h} = 8$ cm.

Fig. 7 shows a sequence of photographs of an experiment which corresponded approximately to the situation of Fig. 2. Dyed water entered through the slot at the upper right and showed the path followed by the water in migrating zonally across the tank, down the western boundary, and zonally across the tank to the exit slot at the eastern wall of the sector. The flow was not as simple as that of the idealized diagram primarily because only 5/6 S_0 passed through the exit slot and 1/6 S_0 was used to raise the level of water in the sector. By the preceding theoretical arguments, there should have been a slow radially inward (poleward) flow over the interior of the tank and this was manifest in the poleward spread of dye from both of the zonal currents. In addition to the southward flowing western boundary current of strength S_0, the theory also predicts an additional component of 1/6 S_0 which is required by continuity and is associated with the distributed sink of 1/6 S_0. This "recirculation" was not made up of source water and must have been drawn from the interior of the basin. We interpret the thin streak of clear water (Figs. 8b, c) between the primary current near the western wall and the poleward flowing mass in the interior as evidence for the "recirculation" flow.

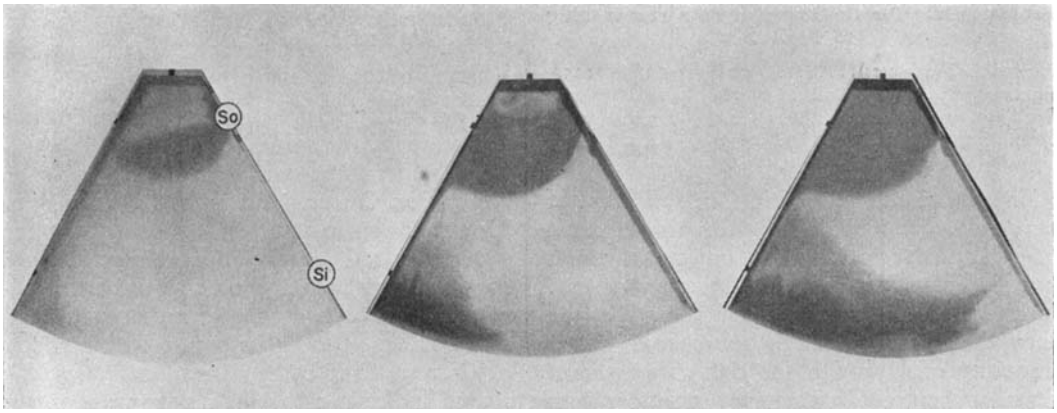

Fig. 7. Photographs at 20, 80, and 220 minutes after the introduction of dye, showing the path followed by the source water ($S_0 = 50$ cc./min.) in flowing from a slot in the eastern wall near the apex to the sink ($S_1 = 5/6\ S_0$) in the same wall near the rim (corresponding to Fig. 2).

Fig. 8 illustrates the circulation with the source at the apex of the sector and with no external sink, i.e., with a uniform rise of the water level in the tank (a uniformly distributed sink). (Compare with Fig. 3 and Case 1. of the mathematical analysis.) In accord with the theory, the interior of the basin filled from the rim and continuity was maintained by an intense western current S_0 from the source, which was augmented by a recirculation (theoretically of strength S_0 for $l = 1$) from the interior water. Evidence for this recirculation is the clear streak in Figs. 8b, c which penetrates toward the rim into the dyed fluid near the western wall. By evaluating the volume of fluid-containing dye, the transport of the total western boundary current has been determined for comparison with the source strength. The data of Table I show that: a) at 20 minutes the dyed fluid was composed almost entirely of source water, b) at 60 minutes the dyed fluid occupied twice the total volume of the input, which implies mixing with an equal volume of clear water (presumably that from the recirculated component of the boundary current), and c) at 125 minutes the dyed volume was less than twice that of the source input, a fact which is consistent with the decrease in the factor l as the mean depth of the fluid ($\bar{h}$) gradually increased. These results are in rough agreement with the quantitative predictions of the theory.

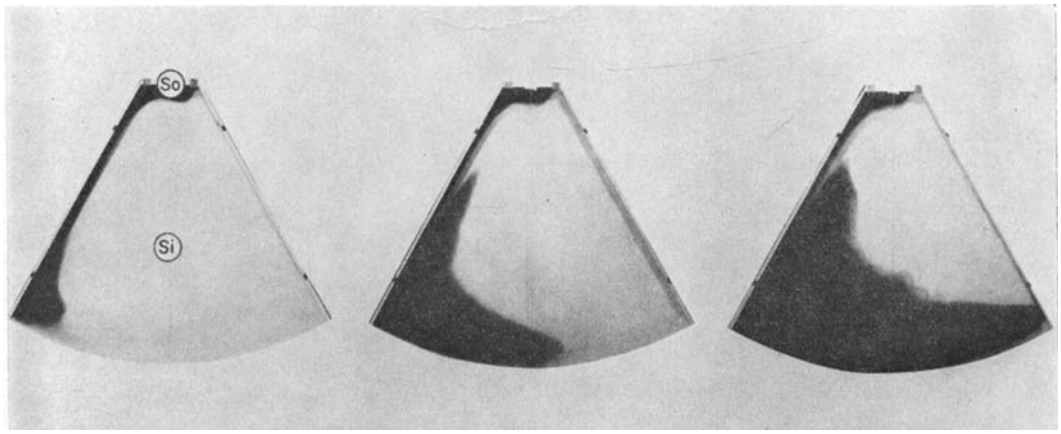

Fig. 8. Photographs at 20, 60, and 80 minutes with $S_0 = 120$ cc./min. The source was at the apex and there was no external sink (corresponding to Fig. 3).

Table 1. Data for the experiment corresponding to Fig. 8.

Elapsed time (minutes).....	20	60	125
Volume with dye (liters).....	1.9	14.6	27.4
Total input from source	2.4	7.2	15.0
Mean depth (h), (cm)	7.7	8.2	10.3

The situations discussed in Cases 2. and 3. of the analysis are illustrated by Figures 9 and 10. In each case the dyed mass was injected through a vertical glass tube in the southwestern cornei. In Fig. 9, with a sink of equal strength at the apex, the greater part of the source mass passed smoothly out through the sink as a western boundary current, except for protuberances caused by inertial oscillations in the tank. (These were the product of slight periodic variations of the rotation rate due to uneven wearing of the driving belt.)

By eliminating the external sink at the apex and allowing the surface to rise slowly (a uniformly distributed sink) as in Fig. 10, we have a situation corresponding to Fig. 4 and to Case 2. of the analysis. Figs. 10b and 10c (three minutes apart) show the rapid southward flowing boundary stream by means of permanganate dye from crystals that were introduced through slits in the glass cover. The intrusion of clear water into the colored mass near the source indicates that the southward flowing current mixed with the source mass, and the

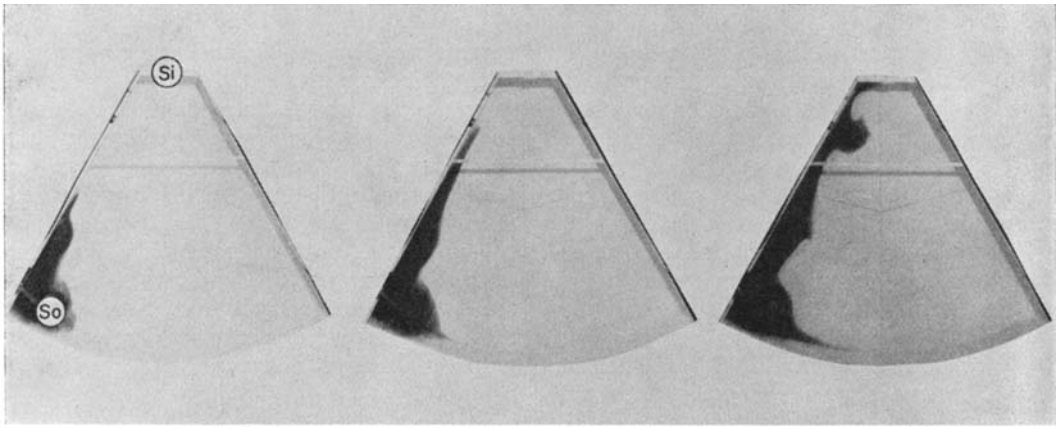

Fig. 9. Photographs at 5, 10, and 20 minutes with $S_0 = 100$ cc./min. The dyed fluid was injected through a vertical glass tube in the southwest corner of the tank and the sink was at the apex.

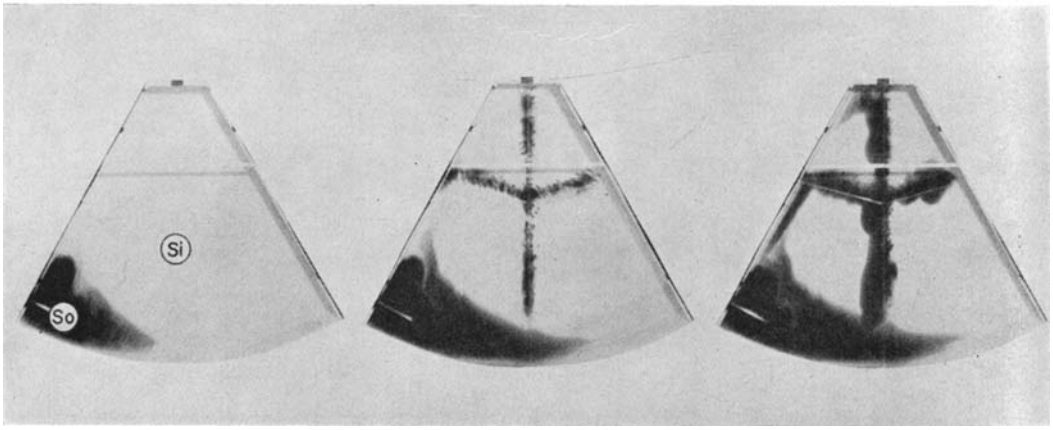

Fig. 10. Photographs at 15, 32, and 35 minutes with $S_0 = 100$ cc./min. This experiment corresponded to fig. 4 and was identical to that of Fig. 9 except that the external sink at the apex was eliminated. Potassium permanganate dye from crystals introduced through slits in the glass cover showed the southward flowing western boundary current.

mixture gradually spread across the tank near the rim. (The anomalous apparent southward flow of permanganate dye in the interior (Fig. 10c) was due to the dense concentration of heavy dye near the botton and antitriptic outward flow toward surfaces of lower "geopotential". The bottom surface of the model was not an equipotential surface, and the introduction of density gradients destroys the simple interpretation of the simulation of the "β" effect by a radial variation of depth.)

REFERENCES

STOMMEL, HENRY, 1957: A survey of ocean current theory. *Deep-Sea Research* **4**, pp. 149-184.

VON ARX W. S., 1952: A laboratory study of the wind-driven ocean circulation. *Tellus*, **4**, pp. 311—318.